# Tube MPC applied to 3SSC boost converter with time-varying parameters disturbance

Rosana C. B. Rego
Department of Engineering and Technology
Federal Rural University of the Semi-Arid Region, Brazil
Email: rosana.rego@ufersa.edu.br

Thalita B. S. Moreira
Graduate Program in Electrical Engineering
Federal Rural University of the Semi-Arid Region, Brazil
Email: thalita_brenna@hotmail.com

Fabricio G. Nogueira
Department of Electrical Engineering
Technology Center, Federal University of Ceara, Brazil
Email: fnogueira@dee.ufc.br

Marcus V. S. Costa
Department of Engineering
Federal Rural University of the Semi-Arid Region, Brazil
Email: marcus.costa@ufersa.edu.br

***Abstract*—This paper proposes an off-line formulation for tube model predictive control (TMPC) with linear matrix inequalities (LMI). The approach involves an off-line set of states. The proposed off-line tube MPC is applied to the three-state switching cell (3SSC) boost converter. A comparison is made between the online and off-line performance of the algorithm. The results showed that the off-line implementation of the tube MPC is possible, and the method is simple, with a very low computational cost, and effective even in the presence of disturbances.**

***Keywords* – Tube MPC, boost converter, time-varying, LMI.**

## I. Introduction

DC-DC converters are widely used in power supply systems, they are considered the most efficient way to implement actuators for electromechanical systems, especially in power electronics structures [1]. The purpose of DC-DC converters is to provide an output DC voltage even when subjected to load or input voltage variations [2].

A DC-DC boost converter has the ability to raise a given DC voltage. It has a simplified topology but presents some singularities in its modeling, such as the variations of load resistance, input voltage and the effects of the non-minimum phase as presented in [3], [4], [5], [6]. Performing the control of these converters is considered a complicated task because the model is non-minimum phase [7], [8].

The model predictive control (MPC) proved to be a very robust control type in most applications, such as in static converters and in electric drive devices. The main causes of this control are that it can be applied either to linear or non-linear multivariate [9], [10], [8], [6].

The MPC is an established method that is well-suited for the control of systems under hard state and input constraints [11]. Its main drawback is the comparatively high online computational effort involved with the evaluation of the control law, as it requires the solution of finite horizon optimal control problems [12]. There are some classifications for MPC: Robust MPC (RMPC) and Tube MPC (TMPC). TMPC is repetitive online utilization of related tube optimal control. But, all RMPC methods result in tubes.

The use of MPC to solve uncertain linear systems have been widely studied in the last decade. Initially proposed by [13] and consolidated by [9], the Robust MPC with Linear Matrix Inequalities (LMIs) approach remains an interesting control technique due to the advantage of guaranteed robust performance, asymptotic stability using Lyapunov function and design tunning through the weighting matrices [14], [15], [16], [17], [18], [19], [20], [21], [22].

On the other hand, the TMPC try to keep the optimal control problems tractable, where the predicted sets are usually over approximated and parametrized by finite dimensional parameters [23], [12]. Recently Tube MPC approach has been extended to nonlinear systems [24], [25], [26], [27].

Most MPC techniques consist of online processes. But, for the implementation of the control in a microcontroller the ideal is to obtain a static gain, that is, constant. However, it ensures the robustness and stability of the system as already discussed in [6], [22].

Thus, this work used the concept of stability ellipsoids, defining a set of points fixed in the ellipsoid, as proposed in [15] and [16]. Using the TMPC technique proposed in [28], we have proposed an off-line formulation for the quasi-min-max algorithm based on the tube MPC technique. The proposed formulation is applied to the three-state switching cell (3SSC) boost converter with time-varying parameters disturbance [8]. The time-varying parameters of the converter considered are the load resistance and input voltage.

Therefore, the paper is organized as follows. First, in Section II, the mathematical modeling of the boost converter and the control strategy is presented. In Section III, the problem is stated and some basic concepts concerning tube MPC are recalled. In Section IV, the numerical example is presented with a comparative analysis between the online and off-line tube MPC. Finally, in Section V, we discuss the conclusions of the study.

**Notation.** *The symbol * is used in some matrix expressions to induce a symmetric structure. For example:*

$$\begin{bmatrix} Q & * \\ S & P \end{bmatrix} = \begin{bmatrix} Q & S^T \\ S & P \end{bmatrix}.$$

*The symbol $\|$ is used to indicate parallel association of resistors. For example:*

$$R_1 \| R_2 = (R_1 R_2)/(R_2 + R_1)$$

## II. Boost converter

Fig. 1 shows the boost converter used [29], [30], [8], [22].

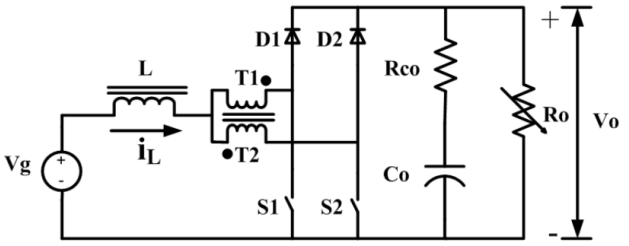


Fig. 1. Boost converter with three-state switching cell.

The parameters used for the converter can be seen in table 1, the same ones used in [31].

TABLE I
Boost converter parameters

| Parameters | Values |
|---|---|
| Input Voltage ($V_g$) | 26-36[V] |
| Output Voltage ($V_o$) | 48[V] |
| Duty Cycle ($D_{cycle}$) | 0.25-0.46 |
| Frequency ($f_s$) | 22[kHz] |
| Inductor (L) | 36[ $\mu H$] |
| Inductive Resistance ($R_L$) | 0 [$\Omega$] |
| Capacitor ($C_o$) | 4400[ $\mu F$] |
| Resistance ($R_{co}$) | 26.7[ $m\Omega$] |
| Resistance ($R_o$) | 2.304-6.06 [ $\Omega$] |
| Output power (Pot) | 380-1000[W] |

### A. Mathematical modeling

The expressions in the state space $A_t$, $B_t$, $C_t$ and $D_t$ operating in Continuous Conduction Mode (CCM) [32] are:

$$\begin{aligned} \dot{x} &= A_t(t)x + B_t(t)u, \\ y &= C_t(t)x + D_t(t)u, \end{aligned} \tag{1}$$

where,

$$A_t = \begin{bmatrix} -\frac{(1-D_{cycle})(R_{co}\|R_o)}{L} & -\frac{(1-D_{cycle})R_o}{L(R_{co}+R_o)} \\ \frac{(1-D_{cycle})R_o}{C_o(R_{co}+R_o)} & -\frac{1}{C_o(R_{co}+Ro)} \end{bmatrix}, \tag{2}$$

$$B_t = \frac{V_g}{R'} \begin{bmatrix} \frac{R_o}{L}\frac{(1-D_{cycle})R_o+R_{co}}{R_o+R_{co}} \\ -\frac{R_o}{R_o+R_{co}} \end{bmatrix}, \tag{3}$$

$$C_t = \begin{bmatrix} (1-D_{cycle})(R_{co}\|R_o) & \frac{R_o}{R_{co}+R_o} \end{bmatrix}, \tag{4}$$

$$D_t = -V_g \frac{R_{co}\|R_o}{R'}. \tag{5}$$

such that $R' = (1-D_{cycle})^2 R_o + D_{cycle}(1-D_{cycle})(R_{co}\|R_o)$, $x = [i_L\ V_c]^T$ where $i_L$ is the inductor current, $V_c$ is capacitor voltage, $u$ is the control signal, $D_{cycle}$ is the duty cycle and $y = V_o$, $V_o$ is the the output voltage.

The uncertainties of the model can be defined by [6], [8]:

$$R_o = f(Pot) = \frac{V_o^2}{Pot} \quad Pot \in [380\ 1000], \tag{6}$$

$$D_{cycle} = f(V_g) = 1 - \frac{V_g}{V_o} \quad V_g \in [26\ 36]. \tag{7}$$

### B. Control strategy

In order to facilitate the analysis, $A_t$, $B_t$, $C_t$, and $D_t$ are discretized and represented by *A, B, C,* and *D*.

In Fig. 2, $g$, $h$ are the matrices that correspond to the degree freedom of the integral action block diagram. $K_i$ and $K$ are respectively the integral action gain and MPC controller gain. $ref$ is the input reference of the system, $y$ is the output of the system. The expressions of the model based on the block diagram are given by,

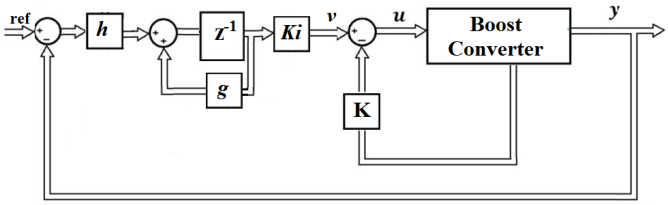


Fig. 2. Block diagram of controller with integral action.

$$\mathcal{A}_i = \begin{bmatrix} A_i & 0 \\ -hC_i & g \end{bmatrix}, \tag{8}$$

$$\mathcal{B}_i = \begin{bmatrix} B_i \\ -hD_i \end{bmatrix}, \tag{9}$$

$$\mathcal{C}_i = \begin{bmatrix} C_i & 0 \end{bmatrix}, \tag{10}$$

whose closed-loop expressions are given by,

$$\bar{\mathcal{A}} = \begin{bmatrix} A_i - B_i K & B_i K_I \\ -h(C_i - D_i K) & g - hD_i K_I \end{bmatrix}, \tag{11}$$

$$\bar{\mathcal{B}} = \begin{bmatrix} 0 \\ h \end{bmatrix}, \tag{12}$$

$$\bar{\mathcal{C}} = \begin{bmatrix} (C_i - D_i K) & D_i K_I \end{bmatrix}, \tag{13}$$

$$\bar{\mathcal{D}} = 0. \tag{14}$$

where $\bar{\mathcal{A}}$, $\bar{\mathcal{B}}$, $\bar{\mathcal{C}}$ and $\bar{\mathcal{D}}$ are the closed-loop matrices whose state is defined by,

$$\hat{x} = \begin{bmatrix} x(k) \\ v(k) \end{bmatrix}, \tag{15}$$

where $v(k)$ is the integral action.

A discrete-time model can be obtained using Euler approximation with a sample time $T_s$ to allow a digital implemantation of the overral scheme:

$$\begin{bmatrix} i_L(k+1) \\ V_c(k+1) \\ v(k+1) \end{bmatrix} = (I + T_s\mathcal{A}) \begin{bmatrix} i_L(k) \\ V_c(k) \\ v(k) \end{bmatrix} + T_s\mathcal{B}u(k),$$

$$y(k) = \mathcal{C} \begin{bmatrix} i_L(k) \\ V_c(k) \\ v(k) \end{bmatrix} \tag{16}$$

## III. TUBE MPC

The idea of Tube MPC is motivated by robustness considerations for system dynamics affected by bounded disturbances. Instead of considering each possible disturbance sequence separately in the prediction (an intractable task), the effect of the bounded disturbances is over-approximated by a sequence of sets which contain all possible state trajectories [12], [28].

The formulation of the tube MPC used are given by the following inequalities, as proposed in [28], [33], [34],

$$\max_{\begin{bmatrix} \mathcal{A}(k+i) & \mathcal{B}(k+i) \end{bmatrix} \in \Omega,\, i \geq 0} J_\infty(k) \leq \leq V(k+i|k) \leq \gamma(k) \tag{17}$$

$$\begin{bmatrix} Q(k) & * & * & * \\ \mathcal{A}_i Q(k) + \mathcal{B}_i Y(k) & Q(k) & * & * \\ \Psi^{1/2} Q(k) & 0 & \gamma(k) I & * \\ R^{1/2} Y(k) & 0 & 0 & \gamma(k) I \end{bmatrix} \geq 0,\ i = 1, ..., L \tag{18}$$

$$\begin{bmatrix} 1 & * & * & * \\ \mathcal{A}(k) z(k) + \mathcal{B}(k) u_z(k) & Q(k) & * & * \\ \Psi^{1/2} z(k) & 0 & \gamma(k) I & * \\ R^{1/2} u_z(k) & 0 & 0 & \gamma(k) I \end{bmatrix} \geq 0, \tag{19}$$

$$\begin{bmatrix} X_{rr} & Y(k) \\ Y^T(k) & Q(k) \end{bmatrix} \geq 0,\ X_{rr} \leq u^2_{r,\max},\ r = 1, 2, \ldots, n_u \tag{20}$$

The difference of this technique to some existing in the literature, is that it assumes a nominal state given by,

$$z(k+1) = A(k) z(k) + B(k) u_z(k). \tag{21}$$

It is noted that the nominal trajectory, the center of the tube, is not a single one. The center trajectory itself is a tube, comprising of infinite possible trajectories, each corresponding to a particular realization. The Fig. 3 illustrate the state evolution, which the solid line is a trajectory of tube center corresponding to a particular realization $[A(k)|B(k)]$ $k \geq 0$, and the grey area is the disturbance invariant tube along a particular tube center [28].

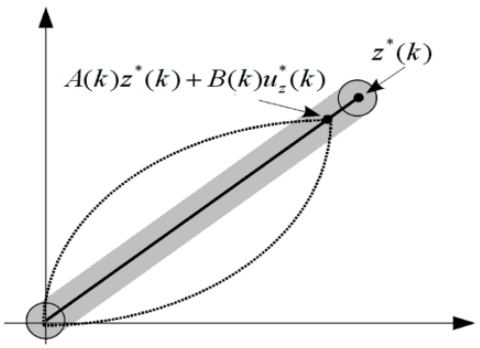


Fig. 3. Illustration of state evolution.

### A. Off-line implementation

To implement the algorithm for tube MPC, do the following: for an off-line system, given an initial condition $z_0$ with $N$, a sequence of minimizers is generated $\gamma_k$, $Q_k$, $U_k$, $Y_k$. Do $k := 1$,

1. compute the minimizers $\gamma_k$, $Q_k$, $U_k$, $Y_k$. Save $Q_k^{-1}$, $K_k$ and $Y_k$ in a *look-up table*.
2. if $k < N$ choose state $z_{k+1}$ satisfying $\|z_{k+1}\|^2_{Q^{-1}} \leq 1$. Do $k := k + 1$ and return to step 1.
   *Drawing the Look-up table:* given an initial condition $\|z_{(0)}\|^2_{Q^{-1}}$, take the state $z(k)$ for the respective time k. Draw the search around $Q^{-1}$ in the *look-up table* to find the highest index $k$ (or equivalent, the smallest ellipsoid $\epsilon = \{z \in \mathbb{R}^{n_x} | \bar{z}^T Q^{-1} \bar{z} \leq 1\}$) so that $\|\bar{z}(k)\|^2_{Q^{-1}} \leq 1$. [16], [6]
3. calculate $K = Y_k Q_k^{-1}$.

## IV. NUMERICAL EXAMPLE

In order to test and compare the effectiveness of the improved off-line tube MPC technique, we used boost convert model described in section II. The circuit implementation considered non-linear continuous modeling using the Runge Kutta $4^{th}$ order method. The initial states of the system (1) is assumed as $x = [38.4615\ \ 26]^T$. The set reference voltage was $V_o = 48V$. The maximum value of the control signal was $u_{max} = 0.5$ and the operating points of the converter is $380W - 1000W$ for sample time $T_s = 1ms$ and simulation step of the $1\mu s$, we used $g = h = 1$. Thus, the system (1) belongs to the following polytope formed by the four local discrete models,

- $f(36V, 1000W)$

$$A_1 = \begin{bmatrix} -0.2838 & -7.7479 \\ 0.0634 & -0.1137 \end{bmatrix}, B_1 = \begin{bmatrix} 580.4780 \\ 65.2800 \end{bmatrix}, \quad C_1 = \begin{bmatrix} 0.0198 & 0.9886 \end{bmatrix}, D_1 = -0.7304. \tag{22}$$

- $f(26V, 1000W)$

$$A_2 = \begin{bmatrix} 0.0958 & -8.4507 \\ 0.0692 & 0.2660 \end{bmatrix}, B_2 = \begin{bmatrix} 851.9920 \\ 53.4470 \end{bmatrix}, \quad C_2 = \begin{bmatrix} 0.0143 & 0.9886 \end{bmatrix}, D_2 = -1.0054. \tag{23}$$

- $f(36V, 380W)$

$$A_3 = \begin{bmatrix} -0.3102 & -7.9646 \\ 0.0652 & -0.1119 \end{bmatrix}, B_3 = \begin{bmatrix} 542.7340 \\ 68.8140 \end{bmatrix},$$
$$C_3 = \begin{bmatrix} 0.0199 & 0.9956 \end{bmatrix}, D_3 = -0.2802. \tag{24}$$

- $f(26V, 380W)$

$$A_4 = \begin{bmatrix} 0.0759 & -8.7329 \\ 0.0715 & 0.02873 \end{bmatrix}, B_4 = \begin{bmatrix} 814.2740 \\ 58.5880 \end{bmatrix},$$
$$C_4 = \begin{bmatrix} 0.0144 & 0.9956 \end{bmatrix}, D_4 = -0.3871. \tag{25}$$

The weighting matrices are

$$\Psi = \begin{bmatrix} 1 & 0 & 0 \\ 0 & 1 & 0 \\ 0 & 0 & 1 \end{bmatrix}, \text{ and } \quad R = 0.1. \tag{26}$$

A step variation of the input voltage of $26V - 36V$ was made, at the time of $0.05s$ and $0.1s$, whose analysis interval was between $0s$ and $0.2s$, as shown in the Figure 4.

The Figures 6 and 5 show the variation of the load ($R_o$) and power ($Pot$) applied in the system simulation. White noise was added to the time-varying parameters to see the controller performance in the presence of noise or disturbance.

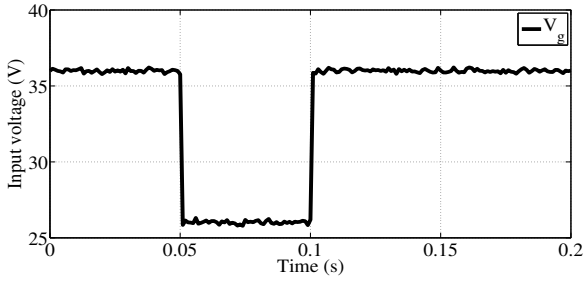


Fig. 4. Variation of the input voltage $V_g$ with disturbances

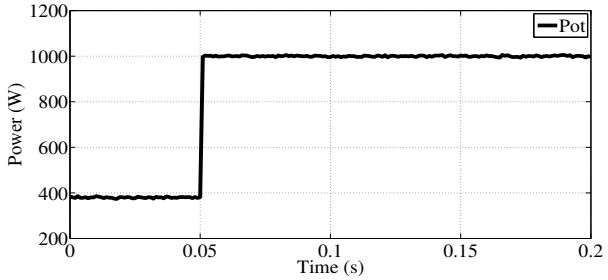


Fig. 5. Variation of the Power $Pot$ with disturbances

The MPC gains $F$ for both online ($F_{on}$) and off-line ($F_{off}$) algorithm are obtained as

$$F_{on} = [\underbrace{0.000123 \ -0.007411}_{K} \ \underbrace{-0.001032}_{K_i}]$$
$$F_{off} = [\underbrace{0.000030 \ -0.003829}_{K} \ \underbrace{-0.001487}_{K_i}]. \tag{27}$$

The gain obtained in the online MPC proposed by [28], ($F_{on}$) is not static, i.e., the gain varies with each iteration. Thus, $F_{on}$ is the gain obtained in the second iteration of the online algorithm. Making N = 20 we have the gain $F_{off}$.

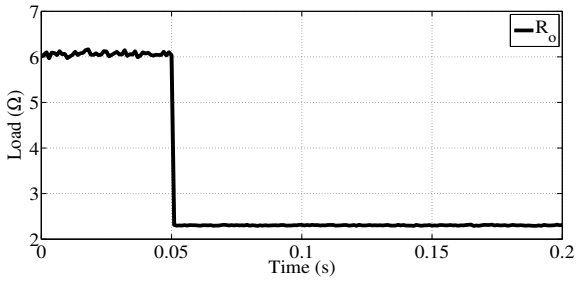


Fig. 6. Variation of the Load $R_o$ with disturbances

In Fig. 7 is shown the stabilization ellipsoids defined by $Q$ for $k = 20$. $Q$ assumes ellipsoidal behavior in the geometric plane and its robust stability is guaranteed with the set $z$ in the steady-state.

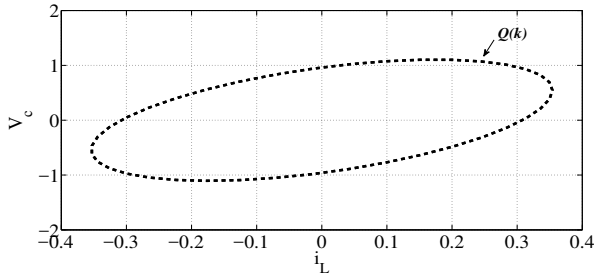


Fig. 7. Stability Ellipsoid Q(k)

Fig. 8 shows the optimal state $z(k)$. It consist in the impulse response defined by $z* = [$ *48.0000 -3.5590 -25.0756 12.5534 8.5864 -10.5746 -0.2914 5.9782 -2.3616 -2.3134 2.2840 0.3170 -1.3984 0.4147 0.5993 -0.4825 -0.1282 0.3213 -0.0646 -0.1506 0.0993*$]$. The impulse response of the boost converter consists of a worst-case condition because its oscillatory characteristic requires more effort from the LMI optimization process so stabilization. However, the optimization process off-line MPC guarantees the stabilization.

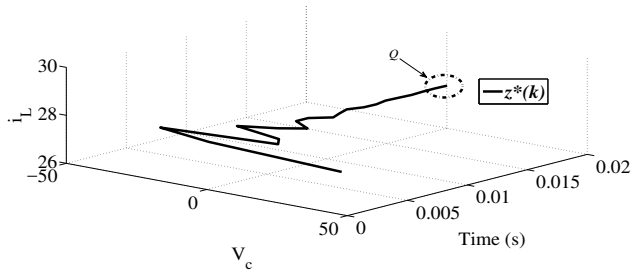


Fig. 8. Stability Ellipsoid and z*(k)

Fig. 9 shows the output voltage ($V_o$). Both controllers followed the preset reference voltage. The online process gives better results in the presence of disturbances. However, in the offline process, where a constant value for $z(k)$ is considered, the system has a faster recovery.

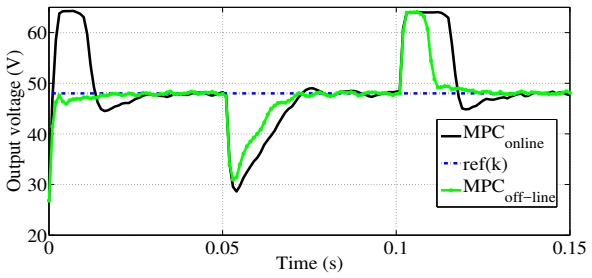


Fig. 9. Output voltage

In Fig. 10 is shown control signal $u(k)$. It is possible to see that for both control techniques the restriction was satisfied. Although a slower response obtained with online. In the off-line the overshoot is considerably reduced.

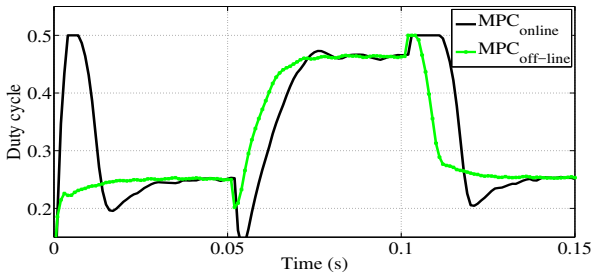


Fig. 10. Control signal

In Fig. 11 the inductor current has a situation similar to the output voltage. Scheme recovery of the system with offline process is faster than the online. Even though all strategies reach an instantaneous peak current of about *105A*.

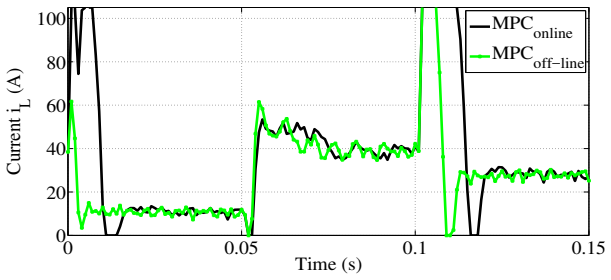


Fig. 11. Inductor current ($i_L$)

Figures 12, 13 and 14 show the simulation results respectively $y(k)$, $u(k)$, and $i_L(k)$ without noise in the time varying parameters. Considering the worst input situation, when $Pot = 1kW$ and $V_g = 26V$, input current should be around $38.5A$, as show in Fig. 14. But, with the presence of noise in time-varying parameters, the inductor current present so much ripple and is between $45A$ and $38.5A$, as shown in Fig. 11.

Moreover, when the input voltage is increased back to $36V$ at $0.1s$ the inductor current has a peak of $105A$. This will certainly be unfeasible in practice and may lead to permanent damage to the converter. So, to avoid the saturation is necessary to apply some technique known as anti-windup [22].

Although the presence of noise in the time-varying parameters causes a lot of ripple in the inductor current, the controller achieved good results.

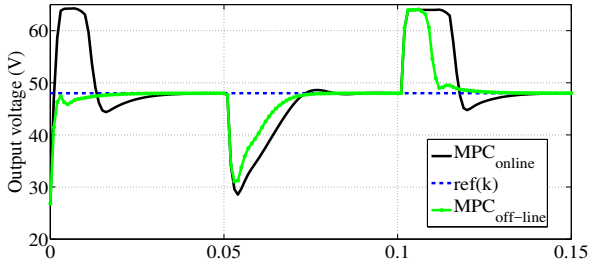


Fig. 12. Output voltage without noise

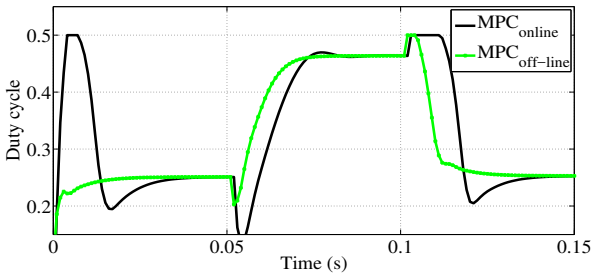


Fig. 13. Control signal without noise

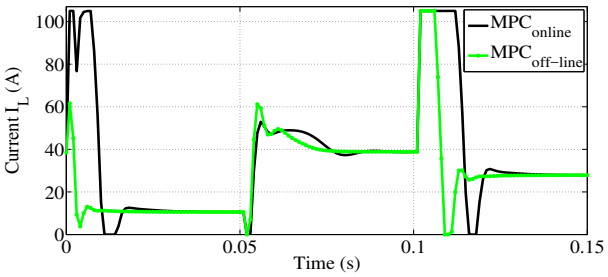


Fig. 14. Inductor current ($i_L$) without noise

## V. Conclusion

Results were presented between the iterative online and off-line processes. Through the simulations, it was seen that the off-line iterative process guarantees the same principles as the robust asymptotic stability of the online process. And also improves the response under time-varying disturbance. The advantage of using the off-line process is that this method does not require as much processing as the online method. Thus, it can be easily applied to an experimental plant such as the boost converter. In our future work, we intend to imposed constraints to avoid the windup effect present in the converter.

## ACKNOWLEDGMENT

The authors would like to thank UFERSA, UFC and CAPES for supported this research. This study was financed in part by the Coordenação de Aperfeiçoamento de Pessoal de Nível Superior - Brazil (CAPES) - Finance Code 001.

## REFERENCES

[1] C. Olalla, R. Leyva, I. Queinnec, and D. Maksimovic, "Robust gain-scheduled control of switched-mode dc–dc converters," *IEEE Transactions on Power Electronics*, vol. 27, no. 6, pp. 3006–3019, 2012.

[2] H. Guldemir, "Modeling and sliding mode control of dc-dc buck-boost converter," in *Proc. 6th Int. advanced technological Symp*, vol. 4, 2011, pp. 475–480.

[3] J. Linares-Flores, A. H. Mendez, C. Garcia-Rodriguez, and H. Sira-Ramirez, "Robust nonlinear adaptive control of a boost converter via algebraic parameter identification," *IEEE Transactions on Industrial Electronics*, vol. 61, no. 8, pp. 4105–4114, 2014.

[4] R. Ortega, J. A. L. Perez, P. J. Nicklasson, and H. J. Sira-Ramirez, *Passivity-based control of Euler-Lagrange systems: mechanical, electrical and electromechanical applications*. Springer Science & Business Media, 2013.

[5] L. Cheng, P. Acuna, R. P. Aguilera, J. Jiang, S. Wei, J. Fletcher, and D. D.-C. Lu, "Model predictive control for dc-dc boost converters with reduced-prediction horizon and constant switching frequency," *IEEE Transactions on Power Electronics*, 2017.

[6] M. V. Costa, F. E. Reis, J. C. Campos *et al.*, "Controlador robusto mpc-lmi aplicado ao conversor boost com célula de comutação de três estados," *Eletrônica de Potência, Campo Grande*, pp. 81–90, 2017.

[7] R. Amirifar, "Extended dynamic matrix control design for a dc-dc power converter," in *System Theory, 2005. SSST'05. Proceedings of the Thirty-Seventh Southeastern Symposium on*. IEEE, 2005, pp. 191–195.

[8] M. V. S. Costa, "Controle mpc robusto aplicado ao conversor *boost* ccte otimizado por inequações matriciais lineares," Thesis, Universidade Federal do Ceará, Fortaleza, 2017.

[9] E. F. Camacho and C. B. Alba, *Model predictive control*. Springer Science & Business Media, 2013.

[10] L. A. Aguirre, A. H. Bruciapaglia, P. E. Miyagi, and J. R. C. Piqueira, *Enciclopédia de automática: controle e automação*. Blucher, 2007.

[11] D. Q. Mayne, J. B. Rawlings, C. V. Rao, and P. O. Scokaert, "Constrained model predictive control: Stability and optimality," *Automatica*, vol. 36, no. 6, pp. 789–814, 2000.

[12] F. A. Bayer, F. D. Brunner, M. Lazar, M. Wijnand, and F. Allgöwer, "A tube-based approach to nonlinear explicit mpc," in *2016 IEEE 55th Conference on Decision and Control (CDC)*. IEEE, 2016, pp. 4059–4064.

[13] M. V. Kothare, V. Balakrishnan, and M. Morari, "Robust constrained model predictive control using linear matrix inequalities," *Automatica*, vol. 32, no. 10, pp. 1361–1379, 1996.

[14] Y. Lu and Y. Arkun, "Quasi-min-max mpc algorithms for lpv systems," *Automatica*, vol. 36, no. 4, pp. 527–540, 2000.

[15] Z. Wan and M. V. Kothare, "Robust output feedback model predictive control using off-line linear matrix inequalities," *Journal of Process Control*, vol. 12, no. 7, pp. 763–774, 2002.

[16] ——, "An efficient off-line formulation of robust model predictive control using linear matrix inequalities," *Automatica*, vol. 39, no. 5, pp. 837–846, 2003.

[17] M. Rodrigues and D. Odloak, "Robust mpc for systems with output feedback and input saturation," *Journal of Process Control*, vol. 15, no. 7, pp. 837–846, 2005.

[18] Y.-Y. Cao and Z. Lin, "Min–max MPC algorithm for LPV systems subject to input saturation," *IEE Proceedings - Control Theory and Applications*, vol. 152, no. 3, pp. 266–272, may 2005.

[19] X. Gao, "Control for ts fuzzy systems based on lmi optimization," Ph.D. dissertation, Dissertation, Jilin University, 2006.

[20] S. Lee, J. H. Park, D. Ji, and S. Won, "Robust model predictive control for lpv systems using relaxation matrices," *IET Control Theory & Applications*, vol. 1, no. 6, pp. 1567–1573, 2007.

[21] Y. Xia, G. P. Liu, P. Shi, J. Chen, and D. Rees, "Robust constrained model predictive control based on parameter-dependent lyapunov functions," *Circuits, Systems & Signal Processing*, vol. 27, no. 4, pp. 429–446, may 2008.

[22] R. C. B. Rego, "Controle MPC robusto com anti-windup aplicado a sistemas LPV e LTV baseado no algoritmo quasi-min-max com relaxação em LMIS," Master's thesis, Federal Rural University of Semi-Arid Region, Brazil, 2019.

[23] S. V. Raković and Q. Cheng, "Homothetic tube mpc for constrained linear difference inclusions," in *2013 25th Chinese Control and Decision Conference (CCDC)*. IEEE, 2013, pp. 754–761.

[24] M. Cannon, Q. Cheng, B. Kouvaritakis, and S. V. Raković, "Stochastic tube mpc with state estimation," *Automatica*, vol. 48, no. 3, pp. 536–541, 2012.

[25] C. Hu, N. Yang, and Y. Ren, "Polytopic linear parameter varying model-based tube model predictive control for hypersonic vehicles," *International Journal of Advanced Robotic Systems*, vol. 14, no. 3, p. 1729881417714398, 2017.

[26] R. Wang and J. Bao, "A differential lyapunov-based tube mpc approach for continuous-time nonlinear processes," *Journal of Process Control*, 2018.

[27] K. M. M. Rathai, J. Amirthalingam, and B. Jayaraman, "Robust tube-mpc based lane keeping system for autonomous driving vehicles," in *Proceedings of the Advances in Robotics*. ACM, 2017, p. 1.

[28] Y. Su, K. K. Tan, and T. H. Lee, "Tube based quasi-min-max output feedback mpc for lpv systems," *IFAC Proceedings Volumes*, vol. 45, no. 15, pp. 186–191, 2012.

[29] G. T. Bascopé and I. Barbi, "Generation of a family of non-isolated dc-dc pwm converters using new three-state switching cells," in *Power Electronics Specialists Conference, 2000. PESC 00. 2000 IEEE 31st Annual*, vol. 2. IEEE, 2000, pp. 858–863.

[30] M. V. S. Costa, "Controladores robustos d-lqi e d-alocação de polos otimizados via lmi aplicados a um conversor boost alto ganho com célula de comutação três estados," Master in Electrical Engineering, Universidade Federal do Ceará, Fortaleza, 2012, 120f.

[31] R. C. B. Rego, M. V. S. Costa, F. E. U. Reis, and R. P. T. Bascopé, "Análise e simulação do controlador mpc-aw-lmi aplicado ao conversor ccte operando em condições de saturação no sinal de controle." *Congresso Brasileiro de Automática*, vol. XXII, 2018.

[32] R. Middlebrook and S. Cuk, "A general unified approach to modelling switching-converter power stages," in *Power Electronics Specialists Conference, 1976 IEEE*. IEEE, 1976, pp. 18–34.

[33] S. V. Raković, B. Kouvaritakis, M. Cannon, C. Panos, and R. Findeisen, "Fully parameterized tube mpc," *IFAC Proceedings Volumes*, vol. 44, no. 1, pp. 197–202, 2011.

[34] M. Cannon, J. Buerger, B. Kouvaritakis, and S. Rakovic, "Robust tubes in nonlinear model predictive control," *IEEE Transactions on Automatic Control*, vol. 56, no. 8, pp. 1942–1947, 2011.